Chemical Physics 382 (2011) 74–79

Contents lists available at ScienceDirect

Chemical Physics

journal homepage: www.elsevier.com/locate/chemphys

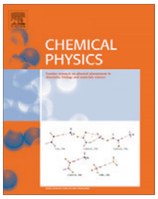

Third-order nonlinear optical properties of a new type of D–π–D unsymmetrical phenoxazinium chloride with resonance structures

Jian-Feng Ge [a,c], Yue-Ting Lu [a], Qing-Feng Xu [a], Wu Liu [a], Na-Jun Li [a], Ru Sun [a,*], Ying-Lin Song [b], Jian-Mei Lu [a,*]

[a] Key Laboratory of Organic Synthesis of Jiangsu Province, Soochow University, Suzhou 215123, China
[b] School of Physical Science and Technology, Soochow University, Suzhou 215006, China
[c] Key Laboratory for Carbon-Based Functional Material and Device of Jiangsu Province, Soochow University, Suzhou 215123, China

ARTICLE INFO

Article history:
Received 30 November 2010
In final form 23 February 2011
Available online 28 February 2011

Keywords:
Phenoxazinium chloride
Third-order NLO
Resonance structure
Z-scan
NLO material
Functional dyes

ABSTRACT

A new series of unsymmetrical phenoxazinium chlorides, featuring a heterocyclic aromatic π-bridge with dialkylamino donors, were evaluated in acetonitrile solution for third-order nonlinear optical properties at 532 nm using a Z-scan technique. The title compounds exhibit strong reverse saturable absorption and nonlinear refraction. The third-order nonlinear optical properties were obtained under nanosecond and picosecond laser beams. The nonlinear mechanism is revealed by the excited-state nonlinearity, as observed from a picosecond pump-probe response experiment for one of the compounds. They are potential nonlinear optical materials because they also have good solubility in polar solvents and good thermal stability.

1. Introduction

Nonlinear absorption materials have attracted extensive attention quite recently due to their different nonlinear absorption processes which have a potential impact on their application in science and technology [1–5]. Organic third-order nonlinear optical (NLO) materials, which can be designed and obtained as specified structures, and possess relatively large nonlinearities and fast response time [6–8], are given special attention. The molecular structural design is based on the empirical models of the aromatic cyclic compounds or conjugated systems (i.e., π-bridges) that may be attached by the donor (D) and/or acceptor (A) groups [9–16].

Large conjugation, donor and/or acceptor substitutions, and recently suggested diradical character are normally the major inducers for significant NLO activity [17]. The large third-order NLO properties of the widely studied centrosymmetric squaraine molecules have been attributed to their D–A–D structure, with their central rings acting as acceptors due to the positive charges localized on several positions around them [18–22]. The corresponding croconate dyes have been proposed to be derivatives of the oxyallyl substructure, such as the squaraine, which would have a larger acceptance capacity due to the positive charges localized on the central ring that may, in turn, lead to more significant NLO activity [23,24]. An oxyallyl-based dye with no central ring, **BM4*i*4*i***, and has large NLO activities was recently reported [24–26]. The large coupling between the two valence bond (VB) resonance structural forms is responsible for the large second hyperpolarizability values [26–29].

To meet these requirements, benzo[a]phenoxazinium salts with resonance structures were recently designed. They demonstrated strong reverse saturable absorption (RSA) and nonlinear refraction with third-order NLO coefficient $\chi^{(3)} = 0.42\text{–}1.20 \times 10^{-11}$ *esu* and the second hyperpolarizabilities $\gamma' = 2.75\text{–}7.29 \times 10^{-29}$ *esu* under a nanosecond laser beam at 532 nm [30]. However, they partially dissociate to the free base and the corresponding acids in highly diluted neutral solvents, which may affect future research. Phenoxazinium chlorides, used for anti-protozoal bioassays [31,32], were selected to eliminate the aforementioned disadvantages. In this paper, six unsymmetrical phenoxazinium chlorides (Fig. 1) were selected and evaluated for their third-order NLO properties. The delocalized D–π–D structure of the phenoxazinium chlorides (**1a–f**) is constructed by a positively charged heterocyclic aromatic bridge and two amino groups as donors, and may be expressed by three stable resonance structures (**i–iii**). The amino groups participated well in the resonance. The presence of the large polarizable conjugated π-electrons in the aromatic heterocycle, as well as the potential electron fluctuant ability, complied with the need for promising third-order NLO materials.

---

* Corresponding authors. Address: College of Chemistry, Chemical Engineering and Materials Science, Soochow University, 199 Ren'ai Road, Suzhou Industry Park, Suzhou 215123, China. Tel.: +86 512 65880368; fax: +86 512 65880367 (J.-M. Lu).

E-mail addresses: sunru924@suda.edu.cn (R. Sun), lujm@suda.edu.cn (J.-M. Lu).

0301-0104/$ - see front matter © 2011 Elsevier B.V. All rights reserved.
doi:10.1016/j.chemphys.2011.02.013

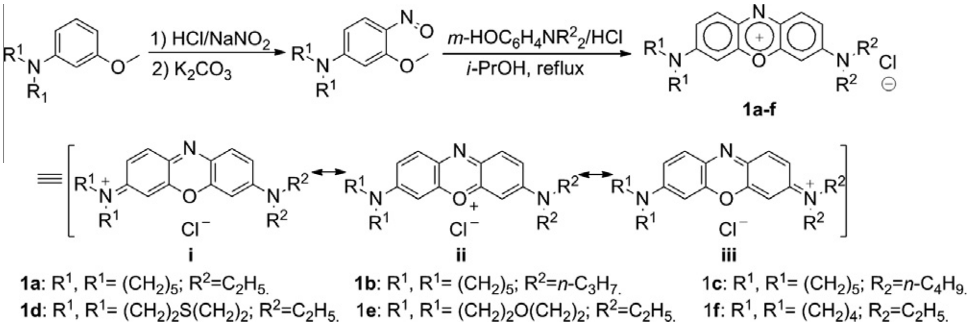

Fig. 1. Synthesis and resonance structures of unsymmetrical phenoxazinium chlorides.

2. Experimental

2.1. Materials

3-(Diethylamino)-7-(piperidin-1-yl)phenoxazin-5-ium chloride (**1a**), 3-(dipropylamino)-7- (piperidin-1-yl)phenoxazin-5-ium chloride (**1b**), 3-(dibutylamino)-7-(piperidin-1-yl)phenoxazin-5-ium chloride (**1c**), 3-(diethylamino)-7-thiomorpholinophenoxazin-5-ium chloride (**1d**), 3-(diethylamino)-7-morpholinophenoxazin-5-ium chloride (**1e**), and 3-(diethylamino)-7- (pyrrolidin-1-yl) phenoxazin-5-ium chloride (**1f**) were synthesized by the reported method (Fig. 1) [31,32]. Their structures are consistent with the reported values by ^{1}HNMR analysis.

2.2. Instruments

Thermogravimetric analyses (TGA) curves were obtained using a Thermo-Gravimetric/Differential Thermal Analyzer (TG/DTA 6300, SII NanoTechnology Inc.). UV–Vis spectra were recorded on a Perkin-Elmer λ-17 spectrometer using a 1 cm square quartz cell.

The third-order NLO properties were measured by the Z-scan technique [33]. An Nd:YAG 532 nm laser (EKSPLA) with a pulse width of 4 ns (fwhm) and a repetition rate of 10 Hz was used for nanosecond Z-scan measurements. A Q-switched Nd:YAG 532 nm laser (EKSPLA) with a pulse width of 21 ps (fwhm) and repetition rate of 2 Hz was used for picosecond Z-scan measurements. The nanosecond Z-scan test of the title compounds (**1a**–**f**) was measured using a 2 mm cell with an incident laser beam energy of 6.2 μJ, while the picosecond Z-scan test was measured using a 2 mm cell with an incident laser beam of 0.4 μJ. Two Rj-7620 energy ratiometers were employed as detectors. The solution was placed in a high-precision mobile platform moving along the direction of the incident light (Z). The Z-scan curve, which is the transmittance as a function of the sample position, may thus be obtained.

In the picosecond pump-probe experiments, a Q-switched Nd:YAG laser (EKSPLA) that delivers 21 ps (fwhm) single pulse at 532 nm with 10 Hz repetition rate was used. The pump–probe experimental setup was a standard arrangement, and the probe peak irradiance was approximately 8% of the pump irradiance [34]. A variable delay was introduced into the probe path, and the two pulses were recombined at the sample cell (2 mm thickness) at a small angle. The probe waist was three times smaller than that of the pump. The small angle between the beams, considering that the probe spot size was noticeably smaller than the pump, ensured that the probe could test a uniformly excited region of material in the 2 mm cell. The polarization of the pump beam was set perpendicular to that of the pump beam to avoid interference. The change in the probe beam intensity as a function of time delay was recorded after the pump beam.

3. Results and discussion

3.1. Structure study with quantum-chemical calculation

To demonstrate an inside view of the unsymmetrical phenoxazinium cation, the structures were fully optimized by using the DFT method for the ground states and the CIS method for the excited states [35]. The basis set used was 6–31G*. Based on the optimized structures, and with the same basis set, vibrational frequencies were calculated. All predicted vibrational spectra have no imaginary frequency, which implies that the optimized geometries were located at the local lowest point on the potential energy surface [36]. All the calculations were performed using the Gaussian 98 program package [37].

The typical molecular orbitals and electric charge distributions of phenoxazinium cation (**1a$^+$**), are given in Fig. 2. The graphics of bonding orbitals clearly demonstrated that the bonding electrons are mainly located in the aromatic phenoxazinium skeleton and the wings of these structures. The conjugations between the two nitrogen atoms and phenoxazinium skeleton are contributed by the orbitals of HOMO-2 and HOMO-5. Comparably, the anti-bonding orbitals are mostly located in the central part of the molecular. From the mapping of Total Charge Density (TCD) with potential, the positive charge is evidently located around the phenoxazinium cation. The unsymmetrical structure with two different amino groups only makes the slight difference for each molecular orbital. The calculated HOMO (eV) and LUMO (eV) energies of phenoxazinium cations (**1a$^+$**–**f$^+$**) are listed in Table 1.

3.2. Solubility and thermal stability

The phenoxazinium chlorides (**1a–f**) have good solubility in most polar solvents, such as water, acetone, chloroform and methanol. Fig. 3 shows their TGA curves in a nitrogen environment at a scan rate of 10 °C · min^{-1}. Their thermal stabilities are comparable, up to approximately 250 °C due to their structural similarity. As seen from the TGA curves, the length of substituted alkyl groups attached to the nitrogen atom has no significant effect on the stability of the phenoxazinium chlorides. It shows that the phenoxazinium chloride is stable enough for organic materials as a low molecular weight organic compound. Both solubility and thermal stability show that the title compounds are promising candidates for optical device process.

3.3. Linear optical properties

The title compounds exhibit absorption maxima in the range of 644–653 nm (Fig. 4). There is only small variation in the absorption maxima with different amino groups. The rigid five member ring (**1f**) has influence the p–π conjugation, the blue shift of this

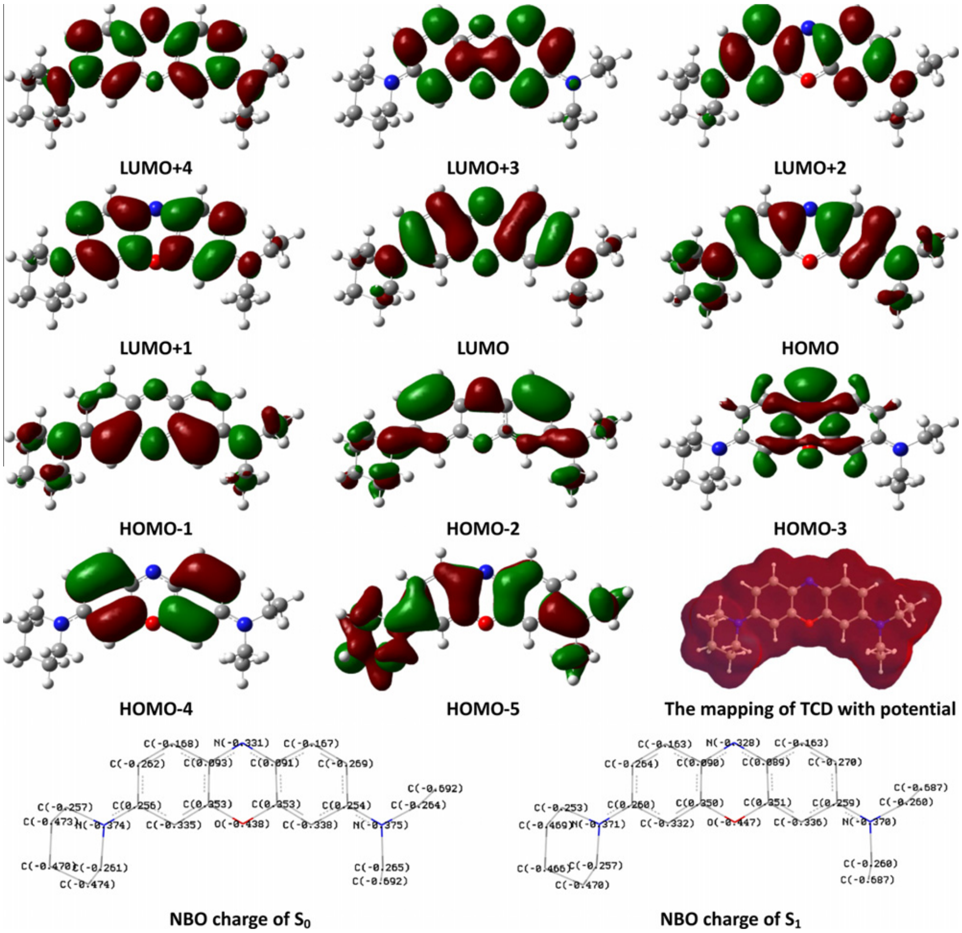

Fig. 2. Molecular orbitals and electric charge distributions of phenoxazinium cation (**1a**$^+$) (TCD: Total Charge Density; NBO: Natural Bond Orbital; S_0: Ground state; S_1: Excited state.)

compound is shown. The absorption maxima are gradually increased (**1e** < **1d** < **1a** < **1b** < **1c**), which is influenced by the electric properties of the donor's abilities of the alkyl groups attached with the nitrogen atoms ($-C_4H_9 > -C_3H_7 > -C_2H_5 > -C_2H_4S > -C_2H_4O$). All the compounds have almost no absorbance at 532 nm, which ensures low intensity and small temperature change for the third-order NLO test [38].

3.4. Nonlinear optical properties

To obtain the second hyperpolarizabilities, the concentration of the title compounds were maintained at $1.79 \times 10^{-4}\ \mathrm{mol \cdot L^{-1}}$ in acetonitrile solution. The nonlinearity of a pure acetonitrile solvent was also measured under the same conditions and no signal could be obtained. Thus, the nonlinearity of the solvent was ignored both under the nanosecond and picosecond laser beams [39,40]. Typical valleys of the normalized transmittance of **1a**, as shown in Fig. 5, indicate that the laser pulses experience strong RSA.

Table 1
Calculated HOMO (eV) and LUMO (eV) energies of phenoxazinium cations.

Entry	Cation	$-R^1$, $-R^1$	$-R^2$, $-R^2$	HOMO (eV)	LUMO (eV)	ΔE_{HL} (eV)
1	**1a**$^+$	$(CH_2)_5$	C_2H_5, C_2H_5	−5.955	−8.408	2.453
2	**1b**$^+$	$(CH_2)_5$	$n\text{–}C_3H_7$, $n\text{–}C_3H_7$	−5.912	−8.353	2.441
3	**1c**$^+$	$(CH_2)_5$	$n\text{–}C_4H_9$, $n\text{–}C_4H_9$	−5.892	−8.326	2.434
4	**1d**$^+$	$(CH_2)_2S(CH_2)_2$	C_2H_5, C_2H_5	−6.097	−8.454	2.357
5	**1e**$^+$	$(CH_2)_2O(CH_2)_2$	C_2H_5, C_2H_5	−6.077	−8.521	2.444
6	**1f**$^+$	$(CH_2)_4$	C_2H_5, C_2H_5	−5.955	−8.434	2.479

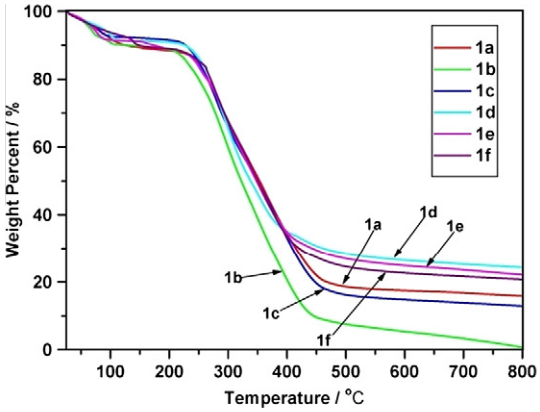

Fig. 3. The thermal stability of the compounds **1a**–**f**.

The nonlinear absorption component was evaluated under an open aperture (OA). Since light transmittance (T) is a function of the sample's Z-position (with respect to the focal point at $Z = 0$), the nonlinear absorption [$\alpha = \beta(I_i)$] and linear absorption (α_0) can be well described by the classical Eq. (1), where α_0 and α are linear and effective third-order NLO absorptive coefficients, respectively. Here, τ is the time and L is the optical path [41–43].

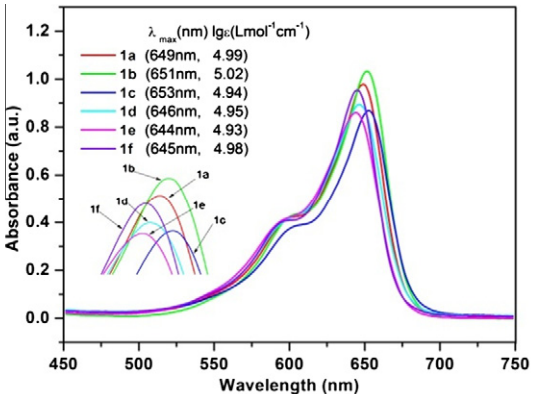

Fig. 4. Linear absorption spectra of **1a–f** in CH_3CN ($c = 1 \times 10^{-5}$ mol · L^{-1}).

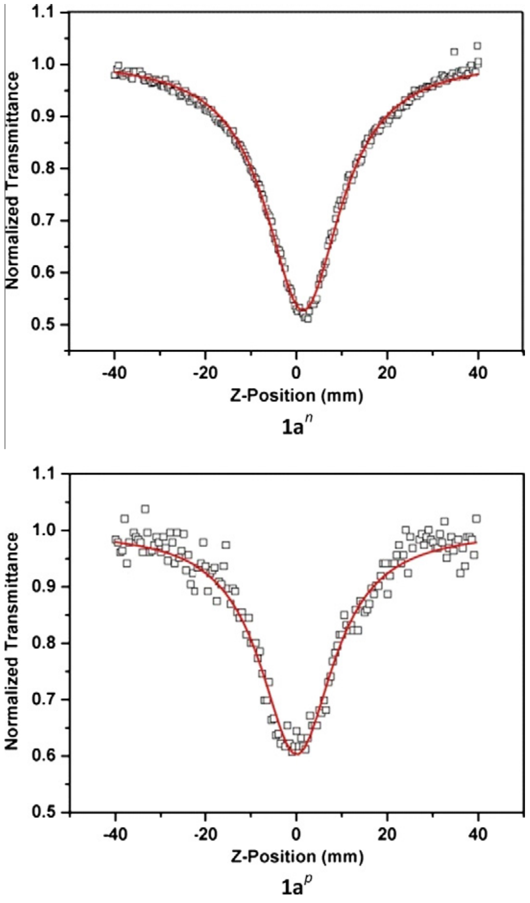

Fig. 5. Z-scan data of OA transmittance for **1a** (^{n}nanosecond, ^{p}picosecond).

$$T(Z) = \frac{\alpha_0}{\sqrt{\pi}\beta I_i(Z)(1-e^{-\alpha_0 L})}\int_{-\infty}^{\infty} \ln\left[1+\beta I_i(Z)\frac{1-e^{-\alpha_0 L}}{\alpha_0}e^{-\tau^2}\right]d\tau. \tag{1}$$

From Fig. 6, for the typical refractive parts of **1a**, the compounds also exhibit strong nonlinear refraction at 532 nm. The nonlinear refractive data were obtained from the ratio of the closed aperture (CA) transmittance divided by the OA transmittance. A positive refractive nonlinearity is observed in Fig. 6, indicating a self-focusing behavior. The valley and peak positions occur at equal distances from the focus. Moreover, the valley–peak separation (ΔZ_{V-P}) and the difference between the normalized transmittance values at valley and peak positions (ΔT_{V-P}) are found to correspond to a set of equations, $\Delta Z_{V-P} = 1.72\pi\omega_0{}^2/\lambda$, and $n_2{}^{eff} = \lambda a_0 \Delta T_{V-P}/[0.812\pi I(1-e^{-\alpha L})]$, which were derived for a third-order NLO process [41,44]. An effective third-order nonlinear refractive index n_2 may be derived from ΔT_{V-P}, where α_0 is the linear coefficient, L is the sample thickness, I is the peak irradiation intensity at the focus, and λ is the wavelength of the laser.

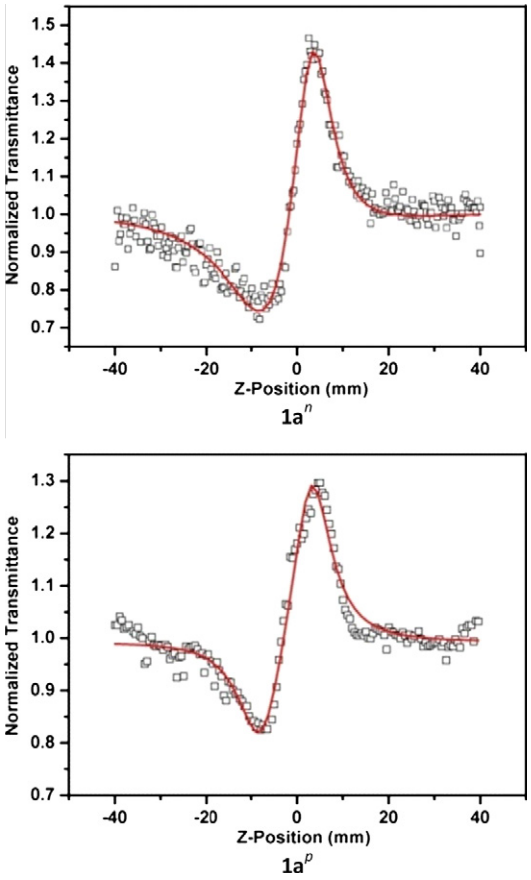

Fig. 6. Z-scan data of refractive parts for **1a** (Data are the ratio of CA/OA transmittance; ^{n}nanosecond, ^{p}picosecond).

From the β and n_2 values, the effective third-order NLO susceptibilities ($\chi^{(3)}$) of the title compounds may be calculated according to the following equations:

$\chi_I{}^{(3)} = 9 \times 10^8 \varepsilon_0 n_0{}^2 c^2 \beta/(4\omega\pi)$, $\chi_R{}^{(3)} = c n_0{}^2 n_2/(80\pi)$, and $\chi^{(3)} = [(\chi_I{}^{(3)})^2 + (\chi_R{}^{(3)})^2]^{1/2}$, respectively [41,45].

The second hyperpolarizabilities (γ') of the compounds were obtained by $\gamma' = \chi^{(3)}/[N((n_0{}^2 + 2)/3)^4]$ [40,41], where N is the density of the molecules in the unit of number of molecules per cm^3, and n_0 is the linear refractive index of the acetonitrile ($n_0 = 1.344$). The third-order NLO properties obtained using nanosecond and picosecond laser beams are listed in Table 2.

The effective $\chi^{(3)}$ and γ' are up to 5.35–8.78 × 10^{-11} and 1.14–8.78 × 10^{-28} *esu* by the nanosecond Z-scan results, while 3.38–4.20 × 10^{-12} and 7.17–8.91 × 10^{-30} *esu* by the picosecond Z-scan results. The data obtained from the former are one order of magnitude or nearly 15 times larger than those from the picosecond Z-scan test. At this point, due to the complexities of the third-order NLO mechanisms, it is difficult to provide a precise explanation for the obtained values. However, it is evident that the energy and frequency of the laser beam and the other conditions affect the effective $\chi^{(3)}$ and γ' values.

The energies of cation's HOMO are somewhat related to the third-order NLO properties in nanosecond test. **1d** and **1f** show

Table 2
NLO properties of **1a–f** in CH_3CN solution.

Entry	Compds.	T_0[c]	*Laser*	n_2 $(10^{-17} m^2 \cdot W^{-1})$	β_{eff} $(10^{-10} m \cdot W^{-1})$	$\chi^{(3)}{}_R$ $(10^{-11}\ esu)$	$\chi^{(3)}{}_I$ $(10^{-11}\ esu)$	$\chi^{(3)}$ $(10^{-11}\ esu)$	γ' $(10^{-29}\ esu)$
1	**1a**	68%	ns[n]	7.33	6.21	6.52	2.34	6.93	14.7
2	**1b**	69%	ns[n]	5.73	5.68	5.09	2.14	5.53	11.7
3	**1c**	68%	ns[n]	5.46	5.93	4.86	2.23	5.35	11.4
4	**1d**	62%	ns[n]	9.33	6.47	8.30	2.44	8.65	18.4
5	**1e**	61%	ns[n]	6.96	5.56	6.19	2.09	6.53	13.9
6	**1f**	67%	ns[n]	9.37	7.26	8.34	2.74	8.78	18.6
7	**1a**	61%	ps[p]	0.403	0.428	0.359	0.161	0.393	0.833
8	**1b**	65%	ps[p]	0.391	0.418	0.347	0.157	0.381	0.808
9	**1c**	60%	ps[p]	0.341	0.397	0.303	0.150	0.338	0.717
10	**1d**	58%	ps[p]	0.402	0.451	0.358	0.170	0.396	0.840
11	**1e**	53%	ps[p]	0.445	0.374	0.395	0.141	0.420	0.891
12	**1f**	57%	ps[p]	0.369	0.413	0.328	0.156	0.363	0.770

[c] Concentration: 1.79×10^{-4} mol L^{-1}.
[n] With nanosecond laser beam at 6.2 μJ, 4 ns.
[p] With picosecond laser beam at 0.4 μJ, 21 ps.

higher γ' in nanosecond test (Table 2, Entry 4, 6), their energies of HOMO (**1d**$^+$, **1f**$^+$) are quite low (Table 1, Entry 4, 6). Antiphonally, higher HOMO energies of **1b**$^+$, **1c**$^+$ (Table 1, Entry 2, 3) lead to the decrease of γ' values (Table 2, Entry 2, 3). **1e**$^+$ (Table 2, Entry 5) has low HOMO energy (Table 1, Entry 5) and relatively low γ' value, probably the result of this compound is influenced by other factors, for example, response time.

Both low HOMO energies and the small energy gaps (ΔE_{HL}) are benefit for the third-order NLO properties in picosecond test. Cations (**1a**$^+$–**b**$^+$, **1d**$^+$–**e**$^+$) with lower HOMO energies and small ΔE_{HL} values (Table 1, Entry 1, 2, 4, 5) show better γ' values of compounds (Table 2, Entry 7, 8, 10, 11), and cations (**1c**$^+$, **1f**$^+$) with higher HOMO energy (Table 1, Entry 3) or big ΔE_{HL} value (Table 1, Entry 3) show slight decline of γ' values (Table 2, Entry 9, 12).

Moreover, the longer alkyl chain attached to nitrogen atom might slightly decrease theirs γ' values (Table 2, Entry 1–3, 7–9) from the results of **1a–c** under nanosecond and picosecond laser beams' data. All the results under nanosecond laser beams are better than the previous reported benzo[a]phenoxazinium salts [30]. The third-order NLO properties of the phenoxazinium chloride reveal that the D–π–D unsymmetrical phenoxazinium chloride with resonance structures is a potential candidate for NLO material.

3.5. Pump-probe measurement

To gain insight into the nonlinear origin of these compounds, picosecond time-resolved pump-probe experiments were conducted at 532 nm on **1a**. The experimental curve is shown in Fig. 7. Initially, the absorption of the solution increases as a function of time, which is consistent with the temporal integration of the pump pulse. The instant drop of the probe is dominant due to the excited singlet absorption, which has a larger cross section than that of the ground state. Once the pump pulse has passed through the sample, the initial response is followed by recovery and the appearance of a long low transmission tail. This behavior is consistent with induced absorption in the first excited singlet state that increases as the excited state is populated, and subsequently diminishes as the population in that state relaxes to the ground state. Hence, the nonlinear mechanism of the compound is typical excited-state nonlinearity [38]. The NBO charge distributions of ground state and excited state for **1a**$^+$ are shown in the Fig. 2. There are only slight changes for the charge distributions of each atoms, that might be a reason for the comparatively stability of the excited state.

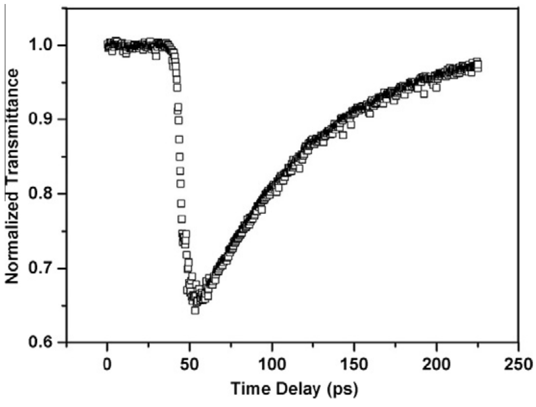

Fig. 7. Pump–probe results for the compound **1a**.

4. Conclusion

In summary, six unsymmetrical phenoxazinium chlorides are selected for the evaluation of third-order nonlinear optical properties. These compounds have potential electron fluctuant abilities with resonance heterocyclic aromatic bridge-donor structural characteristics. The title compounds exhibit strong reverse saturable absorption and nonlinear refraction. The effective third-order NLO susceptibilities ($\chi^{(3)}$) and second hyperpolarizabilities (γ') are up to 5.35–8.78 × 10^{-11} and 1.14–8.78 × 10^{-28} *esu* by nanosecond Z-scan results, while 3.38–4.20 × 10^{-12} and 7.17–8.91 × 10^{-30} *esu* by picosecond Z-scan results. The picosecond pump–probe response of compound **1a** implies that the nonlinear mechanism is of excited-state nonlinearity. The characteristics of solubility and thermal stability indicate they are potential candidates for third-order NLO materials.

Acknowledgments

We thank Professor Masataka Ihara (Hoshi University, Japan) for the encouragements and helpful discussion about the synthesis of title compounds. We are also grateful for financial support from the Natural Science Fund of China (20876101), the Natural Science Fund (BK2009113) and the Natural Science Fund for Colleges and Universities (08KJB430013) in Jiangsu Province.

References

[1] J.E. Ehrlich, X.L. Wu, Y.L. Lee, Z.Y. Hu, H. Rockel, S.R. Marder, J.W. Perry, Opt. Lett. 22 (1997) 1843.
[2] G.S. He, L.S. Tan, Q. Zheng, P.N. Prasad, Chem. Rev. 108 (2008) 1245.
[3] M. Pawlicki, H.A. Collins, R.G. Denning, H.L. Anderson, Angew. Chem., Int. Ed. 48 (2009) 3244.
[4] D.A. Parthenopoulos, P.M. Rentzepis, Science 245 (1989) 843.

[5] S. Kawata, H.B. Sun, T. Tanaka, K. Tanaka, Nature 412 (2001) 697.
[6] T. Kaino, S. Tomaru, Adv. Mater. 5 (1993) 172.
[7] H.S. Nalwa, Adv. Mater. 5 (1993) 341.
[8] J.L. Bredas, C. Adant, P. Tackx, A. Persoons, B.M. Pierce, Chem. Rev. 94 (1994) 243.
[9] G.l. Torre, P. Vazquez, F. Agullo-Lopez, T. Torres, Chem. Rev. 104 (2004) 3723.
[10] H. Rath, J. Sankar, V. PrabhuRaja, T.K. Chandrashekar, A. Nag, D. Goswami, J. Am. Chem. Soc. 127 (2005) 11608.
[11] C. Bucher, C.H. Devillers, J.C. Moutet, G. Royal, E. Saint-Aman, Coordin. Chem. Rev. 253 (2009) 21.
[12] J.A. Delaire, K. Nakatani, Chem. Rev. 100 (2000) 1817.
[13] R.L. Roberts, T. Schwich, T.C. Corkery, M.P. Cifuentes, K.A. Green, J.D. Farmer, P.J. Low, T.B. Marder, M. Samoc, M.G. Humphrey, Adv. Mater. 21 (2009) 1.
[14] M.P. Cifuentes, M.G. Humphrey, J.P. Morrall, M. Samoc, F. Paul, C. Lapinte, T. Roisnel, Organometallics 24 (2005) 4280.
[15] J. Mattu, T. Johansson, G.W. Leach, J. Phys. Chem. C 111 (2007) 6868.
[16] A. Faccinetto, S. Mazzucato, D. Pedron, R. Bozio, S. Destri, W. Porzio, Chem. Phys. Chem. 9 (2008) 2028.
[17] S. Alolse, J. Rehault, B. Moine, O. Poizat, G. Buntinx, V. Lokshin, M. Vales, A. Samat, J. Phys. Chem. A 111 (2007) 1737.
[18] Z. Fushi, Z.K. Kazuo, Chem. Phys. Lett. 441 (2007) 123.
[19] Z.Y. LI, Z.H. Jin, K. Kasatani, H. Okamoto, Chin. Phys. Lett. 22 (2005) 2282.
[20] C.W. Dirk, W.C. Herndon, F. Cervantes-Lee, H. Selnau, S. Martinez, P. Kalamegham, A. Tan, G. Campos, M. Velez, J. Zyss, I. Ledoux, L.T. Cheng, J. Am. Chem. Soc. 117 (1995) 2214.
[21] K. Tran, G.W. Scott, D.J. Funk, D.S.J. Moore, Chem. Phys. 100 (1996) 11863.
[22] J.H. Andrews, J.D.V. Khaydarov, K.D. Singer, Opt. Lett. 19 (1994) 984.
[23] Z. Li, Z.H. Jin, K. Kasatani, H.B. Okamoto, Physica B 382 (2006) 229.
[24] Z. Li, Z.H. Jin, K. Kasatani, H. Okamoto, S. Takenaka, J. Jpn. Appl. Phys. 44 (2005) 4956.
[25] H. Langhals, Angew. Chem., Int. Ed. 42 (2003) 4286.
[26] S. Tatsuura, M. Tian, M. Furuki, Y. Sato, I. Iwasa, H. Mitsu, App. Phy. Lett. 84 (2004).
[27] Y. Orimoto, Y. Aoki, J. Phys. Chem. A 111 (2007) 8241.
[28] H. Fukui, R. Kishi, T. Minami, H. Nagai, H. Takahashi, T. Kubo, K. Kamada, K. Ohta, B. Champagne, E. Botek, M. Nakano, J. Phys. Chem. A 112 (2008) 8423.
[29] K. Yesudas, K. Bhanuprakash, J. Phys. Chem. A 111 (2007) 1943.
[30] B.Q. Liu, R. Sun, J.F. Ge, N.J. Li, X.L. Shi, L.H. Qiu, J.M. Lu, Dyes. Pig. 88 (2011) 50.
[31] J.F. Ge, C. Arai, M. Ihara, Dyes. Pig. 79 (2008) 33.
[32] J.F. Ge, C. Arai, M. Kaiser, S. Wittlin, R. Brun, M. Ihara, J. Med. Chem. 51 (2008) 3654.
[33] C. Zhang, Y.L. Song, X. Wang, F.E. Kühn, Y.X. Wang, Y. Xu, X.Q. Xin, J. Chem. Mater. 13 (2003) 571.
[34] T. Xia, A. Dogariu, K. Mansour, D.J. Hagan, A.A. Said, E.W. Van Stryland, S. Shi, J. Opt. Soc. Am. B 15 (1998) 1497.
[35] C. Lee, W.T. Yang, R.G. Parr, Phys. Rev. B 37 (1988) 785.
[36] W. Li, Q.F. Wu, Y. Ye, M.D. Luo, L. Hu, Y.H. Gu, F. Niu, J.M. Hu, Spectrochim. Acta. A 60 (2004) 2343.
[37] M.J. Frisch, G.W. Trucks, H.B. Schlegel, G.E. Scuseria, M.A. Robb, J.R. Cheeseman, J.A. Montgomery, T.J. Vreven, K.N. Kudin, J.C. Burant, J.M. Millam, S.S. Iyengar, J. Tomasi, V. Barone, B. Mennucci, M. Cossi, G. Scalmani, N. Rega, G.A. Petersson, H. Nakatsuji, M. Hada, M. Ehara, K. Toyota, R. Fukuda, J. Hasegawa, M. Ishida, T. Nakajima, Y. Honda, O. Kitao, H. Nakai, M. Klene, X. Li, J.E. Knox, H.P. Hratchian, J.B. Cross, C. Adamo, J. Jaramillo, R. Gomperts, R.E. Stratmann, O. Yazyev, A.J. Austin, R. Cammi, C. Pomelli, J.W. Ochterski, P.Y. Ayala, K. Morokuma, G.A. Voth, P. Salvador, J.J. Dannenberg, V.G. Zakrzewski, S. Dapprich, A.D. Daniels, M.C. Strain, O. Farkas, D.K. Malick, A.D. Rabuck, K. Raghavachari, J.B. Foresman, J.V. Ortiz, Q. Cui, A.G. Baboul, S. Clifford, J. Cioslowski, B.B. Stefanov, G. Liu, A. Liashenko, P. Piskorz, I. Komaromi, R.L. Martin, D.J. Fox, T. Keith, M.A. Al-Laham, C.Y. Peng, A. Nanayakkara, M. Challacombe, P.M.W. Gill, B. Johnson, W. Chen, M.W. Wong, C. Gonzalez, J.A. Pople, Gaussian 98, Revision A. 5, Gaussian, Inc, Pittsburgh PA, 2003.
[38] J.Y. Yang, J.H. Gu, Y.L. Song, S. Guang, Y.X. Wang, W.H. Zhang, J.P. Lang, J. Phys. Chem. B 111 (2007) 987.
[39] R. Signorini, C. Ferrante, D. Pedron, M. Zerbetto, E. Cecchetto, M. Slaviero, I. Fortunati, E. Collini, R. Bozio, A. Abbotto, L. Beverina, G.A. Pagani, J. Phys. Chem. A 112 (2008) 4224.
[40] M.T. Zhao, B.P. Singh, P.N. Prasad, J. Chem. Phys. 89 (1988) 5535.
[41] M. Sherk-Bahae, A.A. Said, T.H. Wei, D.J. Hagan, E.W. van Stryland, IEEE J. Quant. Electron. 26 (1990) 760.
[42] C. Zhang, Y.L. Song, Y. Xu, H.K. Fun, G.Y. Fang, Y.X. Wang, X.Q. Xin, Dalton Trans. 28 (2000) 23.
[43] Y.Y. Niu, Y.L. Song, H.W. Hou, Y. Zhu, Inorg. Chem. 44 (2005) 2553.
[44] H.W. Hou, Y.L. Wei, Y.L. Song, Y. Zhu, L.K. Li, Y.T. Fan, J. Mater. Chem. 12 (2002) 838.
[45] C. Zhang, Y.L. Song, X. Wang, F.E. Kühn, Y.X. Wang, Y. Xu, X.Q. Xin, J. Mater. Chem. 13 (2003) 571.